# OPTIMIZING PROTEIN PRODUCTION IN THE ONE-POT PURE SYSTEM: INSIGHTS INTO REACTION COMPOSITION AND EXPRESSION EFFICIENCY


## AUTHORS

Yan Zhang,[1] Matas Deveikis,[2] Yanping Qiu,[3] Lovisa Björn,[1] Zachary A. Martinez,[1] Tsui-Fen Chou,[3] Paul S. Freemont, [2] Richard M. Murray[1]

[1] Division of Biology and Biological Engineering, California Institute of Technology, Pasadena, CA, 91125, USA.
[2] Department of Infectious Diseases, Faculty of Medicine, Imperial College London, Exhibition Road, South Kensington, London SW7 2AZ, UK.
[3] Proteome Exploration Laboratory, California Institute of Technology, Pasadena, CA, 91125, USA.



## ABSTRACT

The One-Pot PURE (Protein synthesis Using Recombinant Elements) system simplifies the preparation of traditional PURE systems by co-culturing and purifying 36 essential proteins for gene expression in a single step, thereby improving accessibility and affordability for widespread laboratory adoption and customization. However, replicating this protocol to match the productivity of traditional PURE systems can take considerable time and effort due to uncharacterized variability in the system's biochemical composition. In this work, we observed unstable PURE protein expression in *E. coli* strains M15/pREP4 and BL21(DE3) and addressed this using glucose-mediated catabolite repression to minimize burdensome background expression. We also identified differences in optimal protein induction timing between these two strains, leading to growth incompatibility in co-culture, and observed proteolysis of PURE proteins expressed in M15/pREP4. We showed that consolidating all expression vectors into a protease-deficient BL21(DE3) strain could minimize proteolysis. This single-strain system also led to more uniform cell growth at the time of protein induction, improving the stoichiometry of critical translation initiation factors in the PURE reaction for efficient protein production. In addition to optimizing One-Pot PURE protein composition, we found that variations in commercial energy solution formulations could compensate for suboptimal PURE protein stoichiometry. Moreover, our study revealed significant differences in the expression capacity of commercially available *E. coli* tRNAs, suggesting the potential of optimizing tRNA codons to improve protein translation. Taken together, this work highlights the complex biochemical interplay influencing protein expression capacity in the One-Pot PURE system and presents strategies to improve its robustness and productivity.



## KEYWORDS

PURE system, *in vitro* protein expression, cell-free transcription-translation, synthetic biology

## INTRODUCTION

Cell-free protein expression harnesses the core gene expression machinery in living cells to enable transcription and translation in a test tube reaction. The open nature of these expression platforms allows direct manipulation of the reaction environment. Applications of these platforms span high-throughput screening,[1–3] novel protein modifications,[4,5] interfacing biomolecules with synthetic materials,[6–9] on-demand biosensing[10–12] and biomanufacturing,[13,14] and understanding the rules of life by building biological systems from scratch.[15–18]

Nearly all cell-free protein expression platforms can be categorized into two classes – crude lysate-based and reconstituted systems. Crude lysate-based expression systems use extracts from lysed cells, which retain most of the cell's proteome and metabolic pathways.[19,20] They can support gene expression from a wide range of promoters and enable higher protein expression due to effective energy regeneration.[21] They can also be exceptionally affordable, costing approximately $0.03 per microliter of reaction.[22] However, the active endogenous metabolism and partially intact proteome can divert critical energy sources and metabolites to side reactions, interfering with the central reactions implemented in these systems.[20]

In contrast, the PURE (Protein synthesis Using Recombinant Elements) system isolates the necessary transcription, translation, and energy regeneration proteins to support gene expression by protein purification and reconstitution. This approach creates a more biochemically defined reaction environment, which enables the construction of predictive models for protein expression,[23,24] allows facile removal and replacement of reaction enzymes for customization,[5] and maintains a minimal reaction proteome toward a self-regenerating synthetic cell.[16] However, traditional PURE systems are expensive to purchase ($0.64 – 1.00 per microliter of reaction) and laborious to prepare in-house, posing a significant bottleneck in the broad adoption of PURE systems.

To address these limitations, Lavickova and Maerkl developed the One-Pot PURE system, which offers a simplified alternative.[25] Instead of growing and purifying each of the 36 PURE proteins, they grew a co-culture of the 36 *E. coli* strains, each expressing one of the PURE proteins, and purified the proteins in a single preparation. This approach significantly streamlines PURE system preparation and delivers protein expression yields comparable to commercial PURE systems but at a fraction of the cost ($0.10 per microliter of reaction).

Despite the promise of this method, replicating the One-Pot PURE protocol to achieve productivity comparable to conventional PURE systems can still take considerable time and effort. In this work, we identify sources of variability leading to reduced productivity in One-Pot PURE preparations, including expression instability, suboptimal PURE protein stoichiometry for effective expression, and uncharacterized protease activity during PURE protein purification. Moreover, we demonstrate that variations in the reaction's biochemical composition can also significantly impact the protein production rate and the final protein yield, emphasizing the need for more precise system optimization. Taken together, our findings enhance the current understanding of factors influencing protein expression capacity in the One-Pot PURE system, providing strategies to enable robust and routinized implementation across diverse laboratories and applications.

## RESULTS AND DISCUSSION

### *Enhancing protein expression stability for the One-Pot PURE system through glucose-mediated catabolite repression*

We began by replicating the One-Pot PURE system using plasmids deposited on Addgene and transforming them into the respective *E. coli* expression strains M15/pREP4 and BL21(DE3). Plasmids containing PURE proteins encoded by pQE30 and pQE60 expression vectors were transformed into M15/pREP4 competent cells, with pREP4 plasmid coding for constitutive LacI expression. Plasmids containing PURE proteins encoded by pET21 and pET15 expression vectors were transformed into BL21(DE3) competent cells (**Figure 1A**).

Our initial assessment of protein expression in monoculture assays revealed that several protein expressions were unstable. Despite confirming plasmid sequences through whole plasmid sequencing, we observed a loss of expression in ten proteins after growing and inducing protein expression from saved glycerol stocks (**Figure 1B, C**). No growth defect was observed for these non-expressing cell cultures (**Figure SI.III.1**). This phenomenon was also observed in several expression strains directly obtained from our collaborator, with the loss of protein expression appearing in other strains. This indicates that expression vector instability is a stochastic yet frequent event in PURE protein expression (**Figure SI.III.2**).

The expression vector instability is problematic because previously validated PURE protein expression strains can spontaneously lose protein expression after being saved to and grown from glycerol stocks. Without addressing this issue, subsequent preparations of the One-Pot PURE system may exhibit protein dropouts, leading to unproductive batches. Alternatively, each One-Pot PURE preparation would require fresh transformations of the 36 protein expression vectors, which could be labor-intensive and inefficient. Stabilizing the growth and expression of PURE proteins from glycerol stocks could significantly simplify the preparation workflow and facilitate the dissemination of these strains to other laboratories.

We hypothesize that leaky background protein expression from the $P_{T7\text{-}lacO}$ promoter in BL21(DE3) and $P_{T5\text{-}lacO\text{-}lacO}$ promoters in M15/pREP4 strains can create growth burdens, leading to the loss of protein expression. This phenomenon has been observed by others, in which background protein expression burden led to promoter mutations, resulting in the loss of target protein expression.[5] To reduce background protein expression, we investigated whether catabolite repression – through the addition of a preferred carbon source (glucose) – could upregulate the intracellular concentration of repressors (LacI).[26] This upregulation of LacI repressor could reduce background expression from $P_{T7\text{-}lacO}$ and $P_{T5\text{-}lacO\text{-}lacO}$ promoters.

Indeed, our results showed that by supplementing with growth media with 1% w/v glucose, PURE protein expression was stably maintained even after five serial passages from the seed glycerol stock (**Figure 1D**). For strains grown in catabolite repression media, we also observed improved cell growth and higher protein expression levels in ten PURE proteins previously found to lose expression ability (**Figure SI.III.3**). Based on these findings, all subsequent One-Pot PURE batches were grown with LB media supplemented with 1% w/v glucose.

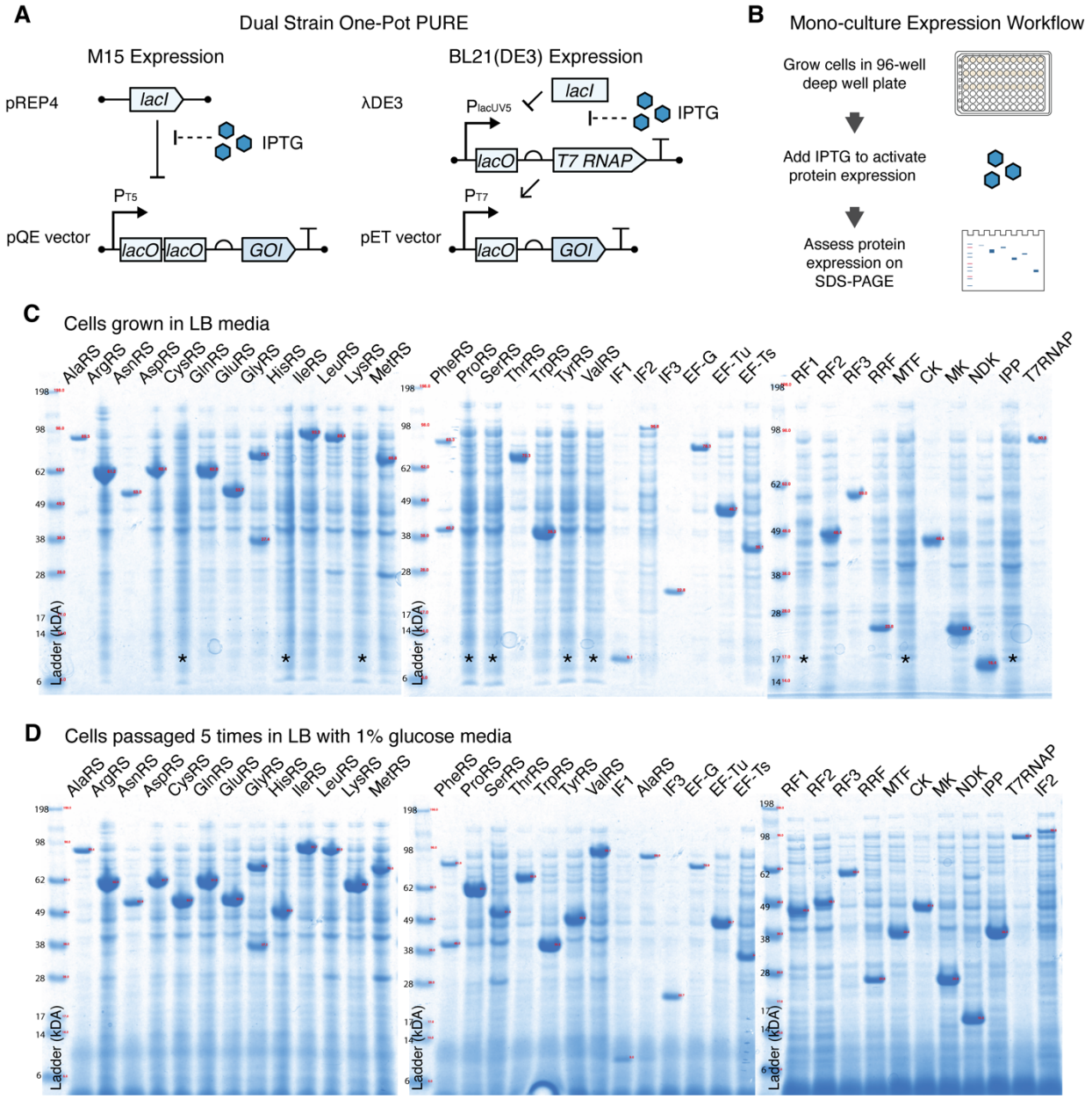


**Figure 1: (A)** Schematic of protein expression and regulation in *E. coli* strains M15/pREP4 and BL21(DE3) for Dual Strain One-Pot PURE systems. Each gene of interest is expressed under the control of either the $P_{T5}$ or $P_{T7}$ promoter followed by lacO operator site(s). In the M15/pREP4 expression strain, the pREP4 plasmid constitutively expresses the *lac* inhibitor, LacI, which represses protein expression by binding to the lacO sites. In BL21(DE3), endogenous LacI represses the production of T7 RNA polymerase (RNAP) and gene expression by binding to the lacO sites. Addition of the IPTG inducer de-represses LacI inhibition and activates gene expression. **(B)** Schematic of monoculture protein expression workflow. Cells were grown in 96-well deep-well plates, and protein expression was activated by adding 0.1 mM IPTG inducer. Following cell growth, protein expression was assessed via SDS-PAGE. **(C)** Monoculture protein expression assessment from cells grown in LB media. Ten strains (designated by *) were found to carry the protein expression plasmid but lacked the protein expression capability. **(D)** Stable protein expression from cells grown in LB with 1% w/v glucose after five serial passages, with all PURE proteins visibly expressed.

126 ***Offsets in the Dual Strain One-Pot PURE protein composition contribute to low protein***
127 ***production.***

128 After resolving the instability in protein expression, we proceeded to replicate the original One-
129 Pot PURE system with BL21(DE3) and M15/pREP4 expression strains (referred to as Dual Strain
130 One-Pot PURE) following the established protocol.[27] To assess the system's transcription and
131 translation capacity, we used a reporter plasmid with a malachite green aptamer (MGA) to
132 approximate mRNA concentration and a green fluorescent protein (deGFP) to measure protein
133 yield (**Figure 2A**). Surprisingly, across two batches of the Dual Strain One-Pot PURE system,
134 while the system produced high mRNA transcripts up to 6 $\mu$M, protein expression was capped at
135 approximately 1.5 $\mu$M (**Figure 2B**). This protein yield is significantly lower than the yield we
136 observed from commercial PURE systems (4-6 $\mu$M, **Figure 3B, Figure 5D**). We also note that
137 the high initial malachite green mRNA concentration at the start of the reaction may have come
138 from rapid mRNA transcription that had begun before the microwell plate was placed into the plate
139 reader.

140 Given that we had confirmed all strains were expressing the One-Pot PURE proteins in mono-
141 culture expression assays, we hypothesized that there might be differences in cell growth or
142 protein expression in the co-culture conditions not captured by the monoculture expression
143 assays. However, using gel electrophoresis to resolve purified One-Pot PURE protein mixture, as
144 done in the monoculture assays, would be challenging due to the similarity in molecular weight of
145 many proteins. We, therefore, used a targeted proteomics approach to characterize the relative
146 abundance of these proteins.

147 Using liquid chromatography with tandem mass spectrometry (LC-MS/MS), we mapped the
148 detected peptides to protein abundances. After scaling for their concentrations in reactions, we
149 compared the relative abundance of individual proteins in the Dual Strain One-Pot PURE mixture
150 to those in commercial PURE systems (**Figure 2C**). Our analysis revealed a consistent deficiency
151 in seven proteins in Dual Strain One-Pot PURE systems compared to the two commercial PURE
152 systems ($PURE_A$ and $PURE_B$). These proteins are alanyl-tRNA synthetase (AlaRS), initiation
153 factor 2 (IF2), initiation factor 3 (IF3), elongation factor-G (EF-G), elongation factor-Tu (EF-Tu),
154 elongation factor-Ts (EF-Ts), and creatine kinase (CK).

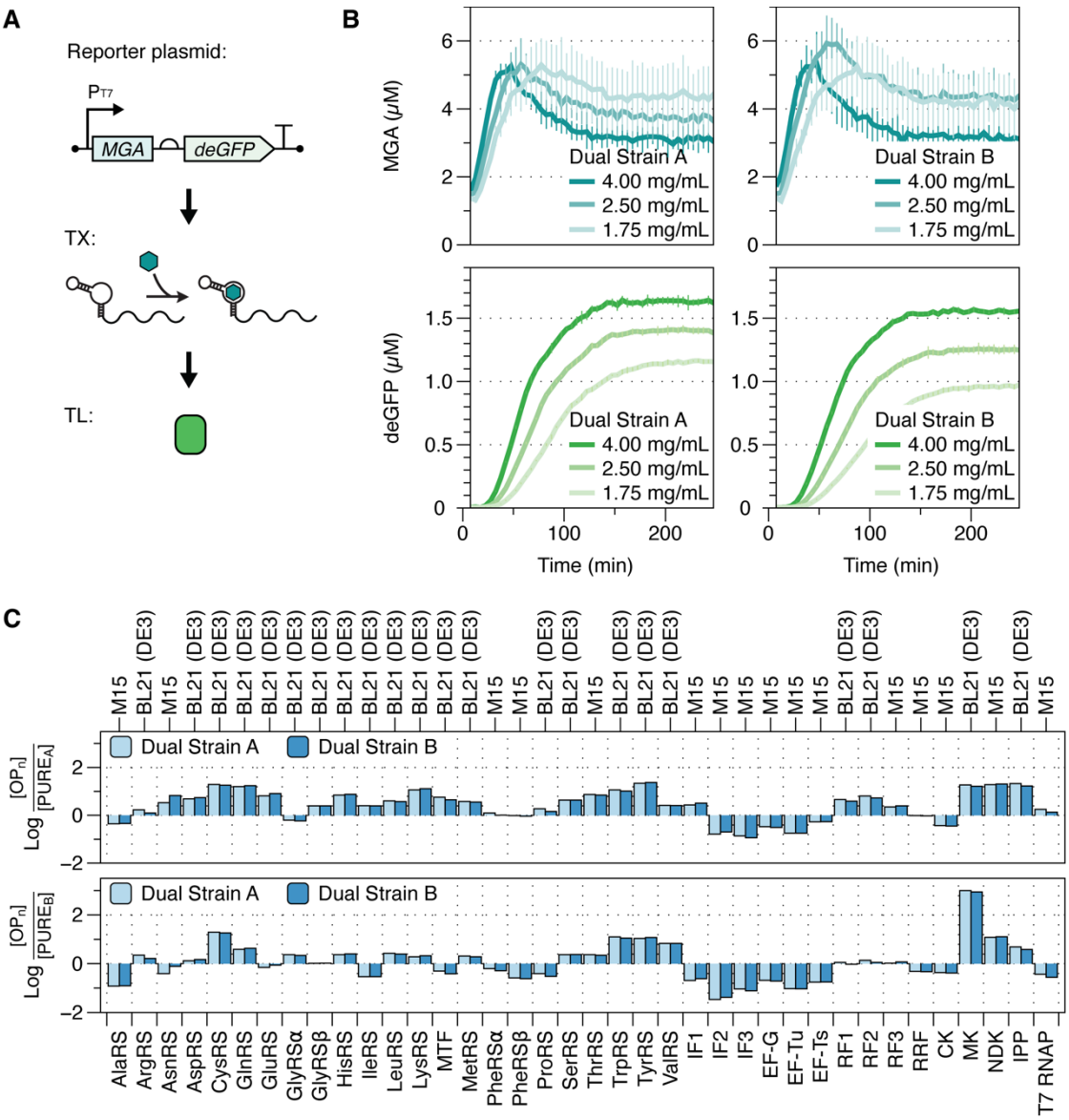


**Figure 2: (A)** Schematic of the reporter plasmid used to assess transcription and translation activity. The plasmid contains an RNA malachite green aptamer (MGA) to assess mRNA transcription and a green fluorescent protein reporter (deGFP) to measure protein expression. **(B)** Productivity of two batches of Dual Strain One-Pot PURE systems (Dual Strain A and Dual Strain B) in transcription and translation, measured via MGA and deGFP, respectively. The One-Pot PURE protein concentration in reactions was varied from 1.75 to 4 mg/mL to optimize protein yield. Plots represent the averages of reaction triplicates, with error bars indicating the standard deviations of reaction triplicates. **(C)** Comparison of protein abundances in Dual Strain One-Pot PURE systems to those in two commercial PURE systems, after scaling by concentrations in the reaction.

164 ***Bypassing Dual Strain One-Pot induction challenge in co-culture with 36-Pot PURE***

165 Since all seven consistently deficient proteins were expressed in the *E. coli* M15/pREP4
166 expression strain, we investigated whether these cells had growth deficiencies. Monoculture
167 growth data revealed that M15/pREP4 cells exhibited slower growth rates than BL21(DE3) cells,
168 and most of them stopped growing after inducing protein expression (**Figures SI.III. 1 and 2**).
169 This mismatch in growth rates created an incompatible induction window when co-culturing
170 BL21(DE3) and M15/pREP4 cells for protein expression. To address this induction incompatibility,
171 we explored growing the strains independently, followed by pooling them together at harvest for
172 purification in a single preparation. We note here that a similar approach has been pursued as
173 part of an open-source PURE protocol.[28]

174 This strategy, named the 36-Pot PURE, involved growing and expressing each of the 36 PURE
175 proteins separately while maintaining the original inoculum composition for One-Pot PURE co-
176 culture. For a 1-L scale preparation, the original One-Pot PURE method requires a 10-mL
177 inoculum consisting of 47% v/v for elongation factor-thermal unstable (EF-Tu) culture and 1.5%
178 v/v of each of the other proteins from saturated overnight cultures. In 36-Pot PURE, thirty-six
179 cultures were grown: one 470 mL for EF-Tu growth culture and thirty-five 15 mL cultures for all
180 other proteins (**Figure 3A**). Each culture was inoculated using a 1:100 dilution of a saturated
181 overnight culture, grown to an induction OD above 0.6, induced for protein expression, and
182 incubated for an additional 3 hours for protein expression.

183 Using this approach, the 36-Pot PURE system showed a twofold increase in deGFP yield
184 compared to the Dual Strain One-Pot PURE system (**Figure 3B**). The improvement may be
185 attributed to the mitigation of growth competition, as growing the strains separately prevented the
186 faster-growing BL21(DE3) strains from outcompeting the M15/pREP4 cells in co-culture. The 36-
187 Pot format also provided more flexibility in selecting optimal induction times for each protein, thus
188 improving the final PURE protein composition. However, despite these improvements, the gene
189 expression capacity still does not match the levels achieved by commercial PURE systems.

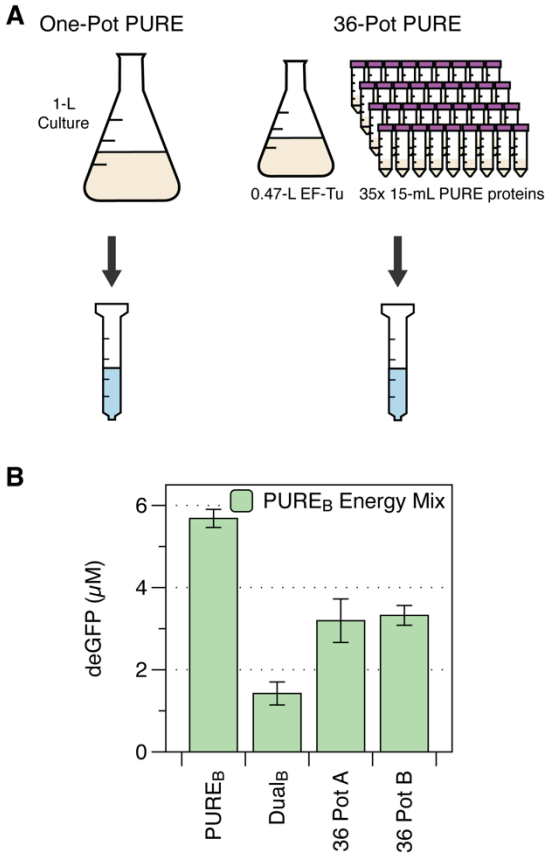


**Figure 3: (A)** Schematic showing the differences in preparation between the Dual Strain One-Pot PURE and 36-Pot PURE system. **(B)** $PURE_B$ is a commercial PURE reaction assembled according to the manufacturer's protocol. Dual Strain One-Pot PURE and 36-Pot PURE reactions were assembled with 5 mg/mL of PURE proteins. All reactions were prepared using a commercial energy solution (supplier B) and contained 5 nM of $P_{T7}$-UTR1-deGFP plasmid. The bar graphs represent the average terminal protein yield of reaction triplicates, with error bars indicating the standard deviations of reaction triplicates.

197 ***T7 RNAP proteolysis in M15/pREP4 expression strain***

198 In a separate attempt to purify T7 RNAP from the M15/pREP4 strain, we discovered protease
199 activity in this expression strain that had not been reported previously. We found that, despite
200 adding a broad-spectrum protease inhibitor (cOMPLETE™) in the lysis buffer, proteolysis of T7
201 RNAP into 80- and 20-kDa fragments was observed after protein purification, suggesting
202 proteolysis occurred during cell lysis (**Figure 4**). This protease activity was not detected in earlier
203 protein gel analyses, where cultures were heat-denatured immediately after protein expression
204 (**Figure 1C, D**).

205 Since M15/pREP4 is not a protease-deficient strain like BL21(DE3), we hypothesize that outer
206 membrane omptin family proteases present in M15/pREP4 were responsible for cleaving T7
207 RNAP into truncated fragments. This is consistent with literature reports that omptins recognize
208 and cleave T7 RNAP into 80- and 20-kDa fragments.[29] Because omptins are aspartyl proteases
209 unaffected by common protease inhibitors,[30] no inhibition of protease activity was observed when
210 lysis buffer was supplemented with Pepstatin A, an aspartyl protease inhibitor. This is consistent
211 with reports of weak inhibition of omptins.[31] In contrast, no proteolysis was observed when T7
212 RNAP was expressed in the BL21/pREP4 strain, which lacks one variant of the omptin family
213 proteases, OmpT (**Figure 4A, B**).

214 It is also possible for omptins to cleave other PURE proteins with similar recognition motifs.[32]
215 Using established omptin cleavage motifs,[33] we identified 12 possible omptin cleavage sites in
216 eight PURE proteins (**Figure 4C**). The susceptible peptides identified for T7 RNAP and creatine
217 kinase (CK) matched literature findings.[32,34] We could not find published results confirming
218 omptin-mediated proteolysis for the other six PURE proteins: myokinase (MK), elongation factor
219 – thermal stable (EF-Ts), and threonyl- (ThrRS), valyl- (ValRS), glycyl- (GlyRS), isoleucyl-tRNA
220 synthetases (IleRS). Using AlphaFold 3 simulations,[35] we found that all but two peptides – one
221 for ValRS and one for IleRS – are located on the external surface of the proteins and are
222 accessible for protease binding (**Figure SI.III. 4**).

223 These simulations suggest that proteolysis of PURE proteins caused by omptins may contribute
224 to the lower gene expression capacity observed during our optimization of the Dual Strain One-
225 Pot PURE system. Since omptins can cleave full-length proteins into truncated fragments, even
226 if these fragments can reassemble and be recovered from affinity column purification, their
227 activities are likely to be reduced, as reported in the case of T7 RNAP.[36]

228 However, we expect the extent of proteolysis to be less significant in the One-Pot PURE and 36-
229 Pot PURE preparation compared to what was observed in this T7 RNAP purification. This
230 expectation arises from the high mRNA transcription activity observed with the Dual Strain One-
231 Pot PURE system in an earlier experiment (**Figure 2A**). We hypothesize that the apparent impact
232 of omptin proteolysis on the protein expression capacity of the Dual Strain One-Pot PURE and
233 36-Pot systems may be reduced by extra copies of T7 RNAP produced by BL21(DE3) cells and
234 a lower abundance of omptins in the cell mixture with BL21(DE3) cells.

235 We also note that the M15/pREP4 strain was not used in the original development of the PURE
236 system. All proteins were expressed in BL21/pREP4 and BL21(DE3) strains lacking the OmpT
237 protease.[37] As a result, we find it is critical to transfer all PURE protein expressions to a protease-
238 deficient strain to ensure the production of full-length, active PURE proteins.

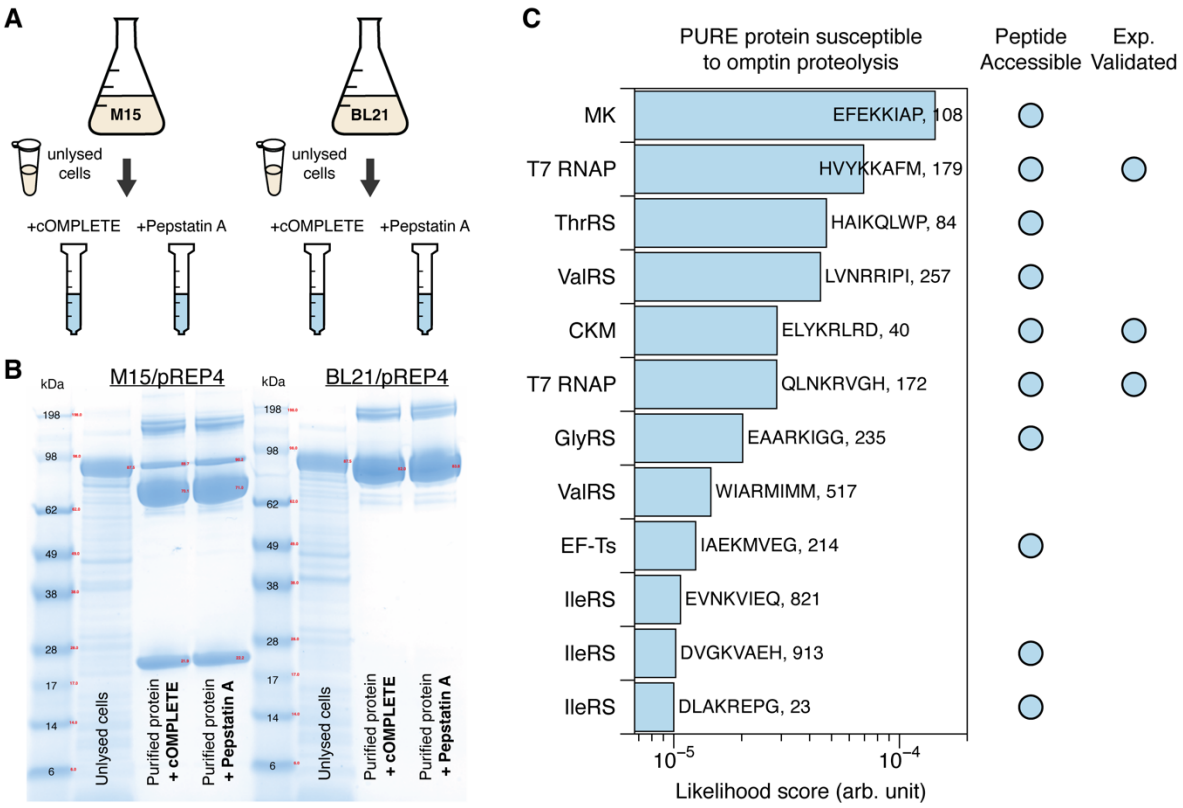


**Figure 4: (A)** Schematic of T7 RNAP preparation to assess outer membrane omptin family protease activity present in M15/pREP4 and BL21/pREP4 strains. A single culture of cells was grown, induced for T7 RNAP expression, and harvested, following a procedure similar to One-Pot PURE co-culture preparations. An un-lysed aliquot of cells expressing T7 RNAP was saved for SDS-PAGE analysis. The cultures were then split into two lysis and purification groups, each treated with a different protease inhibitor (cOMPLETE™ and Pepstatin A). **(B)** SDS-PAGE gel result showed T7 RNAP proteolysis when grown and purified in M15/pREP4 strains. Omptin proteases cleaved full-length T7 RNAP into truncated 80- and 20-kDa fragments. Proteolysis of T7 RNAP is absent in the BL21/pREP4 strain, which is deficient in the OmpT protease. **(C)** Simulated likelihood score of PURE proteins with peptide-subsequences susceptible to omptin proteolysis. The identified peptide sequences were assessed for their accessibility for omptin proteolysis (**SI. III. Figure 4**) and compared with existing literature. Only peptides for T7 RNAP and creatine kinase (CK) matched literature findings.[32,34]

251 ***Enhancing One-Pot PURE protein composition and expression capacity with a Single-***
252 ***Strain One-Pot PURE system***

253 To prevent unwanted proteolysis and attain more uniform cell growth in the co-culture
254 environment, we transferred all PURE proteins encoded in the pQE30 and pQE60 vectors for
255 M15/pREP4 expression to pET21 vectors for BL21(DE3) expression. However, a caveat of this
256 Single Strain One-Pot PURE system is that the T7 RNAP needs to be removed from the One-Pot
257 PURE co-culture due to the genetic instability of having a $P_{T7}$ promoter expressing T7 RNAP. As
258 a result, we opted to purify and add T7 RNAP into One-Pot PURE reactions separately (see
259 **MATERIALS AND METHODS**). Alternatively, T7 RNAP could be co-transformed with pREP4
260 plasmid carrying constitutive LacI expression into BL21 cells and grown in the One-Pot PURE co-
261 culture.

262 Our results showed that five out of the 16 proteins previously expressed in M15/pREP4 cells
263 exhibited at least a 30% improvement in expression levels when grown in BL21(DE3) cells, as
264 determined by monoculture growth and SDS-PAGE analysis (**Figure SI.III. 5**). This enhancement
265 is also evident in the Single Strain One-Pot PURE co-culture. Compared to the Dual Strain system,
266 the purified PURE protein mixture from the Single Strain system has a slightly higher composition
267 of translation factors (24% and 26% for Dual Strain and Single Strain, respectively, **Figure 5B**).
268 Using mass spectrometry to resolve individual protein composition, we found that translation
269 initiation factors 2 and 3 (IF2 and IF3) and creatine kinase (CK) involved in energy regeneration
270 (**Figure 5A**) are present at significantly higher concentrations in Single Strain One-Pot PURE. An
271 Individual protein composition comparison of Single Strain One-Pot PURE to commercial PURE
272 systems is also provided in **Figure SI.III. 6**.

273 We next compared the productivity of the Dual Strain and Single Strain versions of the One-Pot
274 PURE system. Using only the energy solution from commercial vendors and replacing commercial
275 PURE proteins with One-Pot PURE proteins, we observed consistently higher protein production
276 with the Single Strain One-Pot PURE system (**Figure 5C, D**). The robustness of the Single-Strain
277 system was further validated through a reproducibility study conducted in our collaborator's lab.
278 A new batch of Single Strain One-Pot PURE system was prepared following the same protocol
279 (referred to as $Single_C$), and its productivity was compared to shipped aliquots of previous batches,
280 $Single_B$ and $Dual_B$. Even in a different laboratory setting, using separate equipment and reaction
281 consumables, the higher yield of the Single Strain system was reproduced on the first attempt.
282 This was observed both with commercial energy systems (**Figure 5E**) and with homemade energy
283 solutions (**Figure SI.III. 7**)

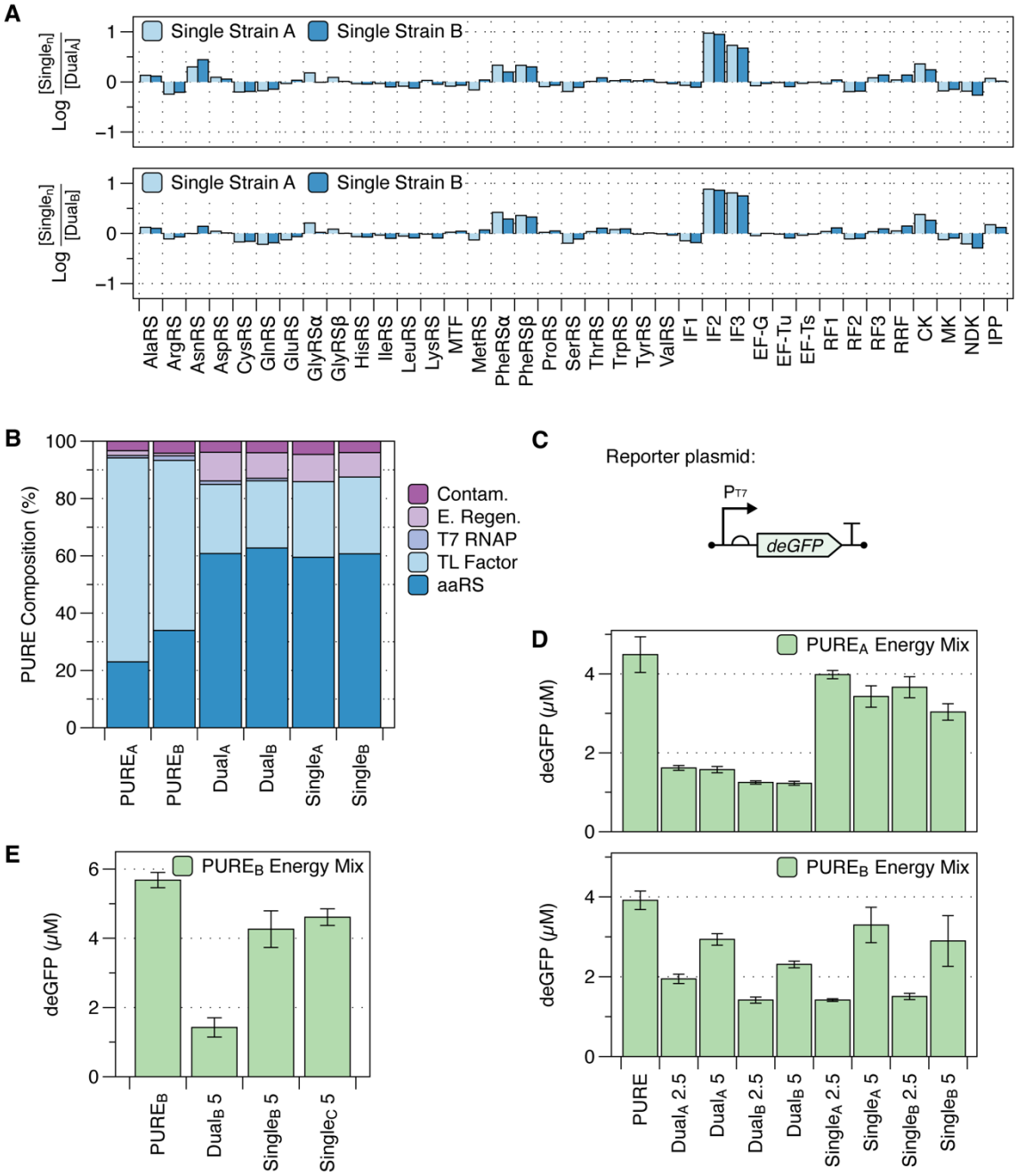


**Figure 5: (A)** Comparison of the relative abundance of individual One-Pot PURE proteins in the Single Strain and Dual Strain systems. Initiation factors 2 and 3 (IF2, IF3) show the most notable increase in composition in the Single Strain One-Pot PURE system. Previously under-expressed aminoacyl-tRNA synthetases (AlaRS and PheRS) and creatine kinase (CK) also increased in composition in the Single Strain One-Pot PURE system. **(B)** Composition of commercial PURE proteins, Dual Strain One-Pot PURE proteins, and Single Strain One-Pot PURE proteins grouped by protein classes: aminoacyl-tRNA synthetase (aaRS), translation factors (TL factors), T7 RNAP, energy regeneration (E Regen.). Detected proteins not part of the PURE proteins are categorized as contaminants (Contam.). Ribosomal proteins are excluded from the analysis. **(C)** Schematic of the reporter plasmid $P_{T7}$-UTR1-deGFP expressed in PURE reactions to assess system productivity. **(D)** Productivity of Dual Strain and Single Strain One-Pot PURE reactions assembled with two commercial energy solutions. $PURE_A$ and $PURE_B$ are control reactions with 5 nM $P_{T7}$-UTR1-deGFP plasmids assembled according to the manufacturer's protocol. "$Dual_n$ 2.5" and "$Dual_n$ 5" designate varying batches of Dual Strain One-Pot PURE proteins added at 2.5 and 5 mg/mL. Likewise, "$Single_n$ 2.5" and "$Single_n$ 5" designate

297 varying batches of Single Strain One-Pot PURE proteins added at 2.5 and 5 mg/mL. The bar graphs represent the
298 average terminal protein yield of reaction triplicates, with error bars indicating the standard deviations of reaction
299 triplicates. **(E)** Productivity comparison of the collaborator's batch of Single Strain One-Pot PURE ($Single_C$). $PURE_B$ is
300 the control reaction assembled according to the manufacturer's protocol. Single Strain and Dual Strain One-Pot PURE
301 reactions were assembled using 5 mg/mL of PURE protein, using the commercial energy solution from supplier B and
302 5 nM of $P_{T7}$-UTR1-deGFP plasmid. The bar graphs represent the average terminal protein yield of reaction triplicates,
303 with error bars indicating the standard deviations of reaction triplicates.

***High-yield protein expression from One-Pot PURE requires a balance between the protein production rate and energy solution formulation.***

The differences in productivity between the Dual Strain One-Pot PURE system when using two commercial PURE energy solutions, referred to as $PURE_A$ and $PURE_B$, are particularly interesting. It appears that higher amounts of One-Pot PURE proteins can be added in reactions with $PURE_B$ energy solution as a strategy to compensate for a sub-optimal stoichiometry of translation factors in the purified protein mixture (**Figure 5D**). In reactions with the $PURE_A$ and homemade energy solution, increasing the concentration of One-Pot PURE proteins from 2.5 mg/mL to 5 mg/mL decreased protein production.

Although we do not know the exact formulation of these energy solutions, comparing the protein production rates (coupled transcription-translation rates) of One-Pot PURE systems to commercial PURE systems provides valuable insights (**Figure 6** and **Figure SI.III 8-9**). In the $PURE_A$ energy solution, the protein production rates of the Dual Strain and Single Strain One-Pot PURE systems reflected the anticipated PURE protein differences based on their translation factor content (**Figure 6**). Deficiencies in translation factors in the Dual Strain One-Pot PURE system contributed to a lower production rate over the course of the reaction. With more protein translation machinery, the Single Strain One-Pot PURE system could match or even exceed the production rate of commercial $PURE_A$ proteins. However, higher production rate peaks led to steeper rate declines shortly after, as observed for the Single Strain One-Pot PURE system with the $PURE_A$ energy solution.

In the $PURE_B$ energy solution, when both the Dual Strain and Single Strain One-Pot PURE proteins are added to 5 mg/mL, both systems exhibited comparable protein expression levels despite the deficiency in translation factors found in the Dual Strain One-Pot PURE proteins (**Figure 6**). It is important to note that the contribution to these differences in translation rate comes from the energy solution alone (amino acids, NTPs, tRNA, creatine phosphate, and other co-factors). All reactions were assembled with the same reporter plasmids and ribosomes. This result suggests that an optimal preparation of the energy solution could compensate for an otherwise sub-optimal One-Pot PURE protein stoichiometry in reactions.

We found it intriguing that when the production rate from the One-Pot PURE system exceeded that of commercial PURE proteins, a steeper drop in production rate soon followed (**Figure 6**). We first attempted to explain the phenomenon from the perspective of the system's energy regeneration capability. While fast protein production can occur, it can also significantly deplete the available energy molecules (ATP and GTP) critical for powering translation initiation and elongation reactions. A fast production rate surpassing the system's energy regeneration capacity can negatively impact the final protein yield by stalling protein translation, potentially resulting in premature translation termination and lower apparent protein production. This corroborates the finding that supplementing an additional energy regeneration system to the PURE reaction can help attain a higher maximum protein production rate.[38]

However, the energy regeneration bottleneck can only explain the protein production behavior observed in reaction with $PURE_A$ energy solution and Single Strain One-Pot PURE proteins. If energy regeneration was the only bottleneck in protein production, then reactions with suboptimal PURE protein stoichiometry (Dual Strain One-Pot PURE) should have a lower yet longer-lasting maximal protein production rate in the $PURE_A$ energy solution. Similarly, energy regeneration

alone cannot explain the discrepancy between the Dual Strain and Single Strain One-Pot PURE expression behaviors in $PURE_A$ and $PURE_B$ energy solutions.

These observations lead us to consider additional factors contributing to differences in protein expression rates. One component often overlooked in optimizing cell-free expression capacity is the tRNA composition and codon usage. Because the exact tRNA composition for each codon in the PURE reaction is not known, and protein translation is influenced by codon usage, it is often challenging to optimize the expressed protein's codon usage to the tRNA composition in the reaction.

Since the same reporter plasmid was used for Dual Strain and Single Strain One-Pot PURE reactions in different PURE energy solutions, the differences in final yield and maximal production rate may be influenced by the tRNA codon composition in different energy formulations. We hypothesize that a sub-optimal tRNA composition in the reaction, not matching well with the codon usage of the reporter protein, may also contribute to ribosome stalling on the mRNA transcript when encountering sub-optimal codons.[39] This could be exacerbated by an mRNA transcript with a high translation initiation rate, such as the one used in the reporter plasmid (UTR1 ribosomal binding site),[40] which increases the frequency of ribosomal collisions. Colliding ribosomes could lead to ribosomal fall-off, resulting in a low apparent yield of protein translation. This also corroborates with reports of C-terminal truncated protein produced in PURE reactions.[41]

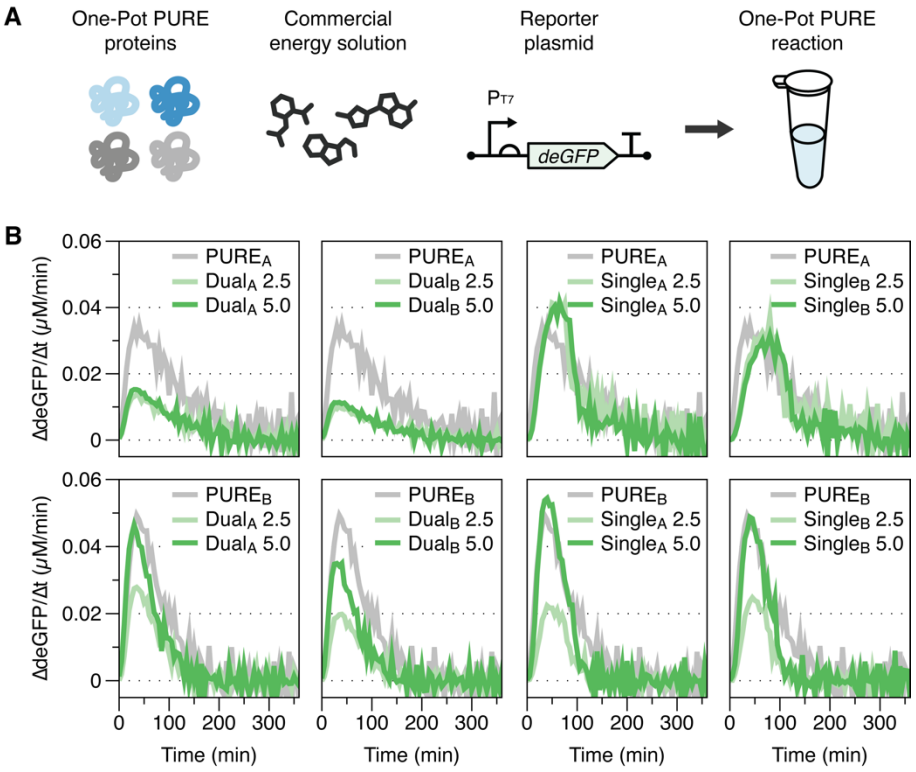


**Figure 6: (A)** Schematic of One-Pot PURE reaction composition using Dual Strain and Single Strain One-Pot PURE proteins with commercial energy solutions, assembled according to manufacturers' protocols. All reactions used 5 nM of $P_{T7}$-UTR1-deGFP reporter plasmid. In the case of Single Strain One-Pot PURE reactions, 0.5 $\mu$M of purified T7 RNAP was added. **(B)** Comparison of protein translation rate for various preparations of One-Pot PURE proteins (added to the reaction at 2.5 or 5.0 mg/mL) using two commercial energy solutions. Plots represent the average of reaction triplicates. Time traces of deGFP production are provided in the **Supplementary Figures SI.III. 8-9**.

372 ***E. coli tRNA composition critically influences One-Pot PURE reaction productivity.***

373 We further demonstrated the important influence of suboptimal tRNA composition on protein
374 production by preparing homemade energy solutions using two different sources of commercial
375 *E. coli* tRNA mixtures: one from *E. coli* strain MRE600 and one from *E. coli* strain W. In these
376 experiments, the same concentrations of the Single Strain One-Pot PURE proteins, reporter
377 plasmids, ribosomes, and T7 RNAP were used. The only difference between the reactions was
378 the source – and possibly the composition – of *E. coli* tRNA in the energy solution.

379 It was observed that the energy solution prepared using *E. coli* MRE600 tRNA exhibited a high
380 protein production rate and final protein yield (**Figure 7B**). When we replaced tRNA in the energy
381 solution with *E. coli* Strain W tRNA, we observed a significant decrease in protein production rate
382 and yield (**Figure 7C**). Increasing the concentration of *E. coli* Strain W tRNA did not improve the
383 rate and yield of protein expression.

384 This finding is significant because the complexity and composition of tRNAs can be overlooked
385 when preparing the energy solution for PURE reactions. Differences in codon usage among
386 various *E. coli* strains can lead to unexpected deficiency in tRNAs associated with the codons
387 used. Without prior knowledge of these tRNA deficiencies, it can be difficult to codon-optimize the
388 protein for effective expression, resulting in low apparent protein yield despite an otherwise
389 productive system.

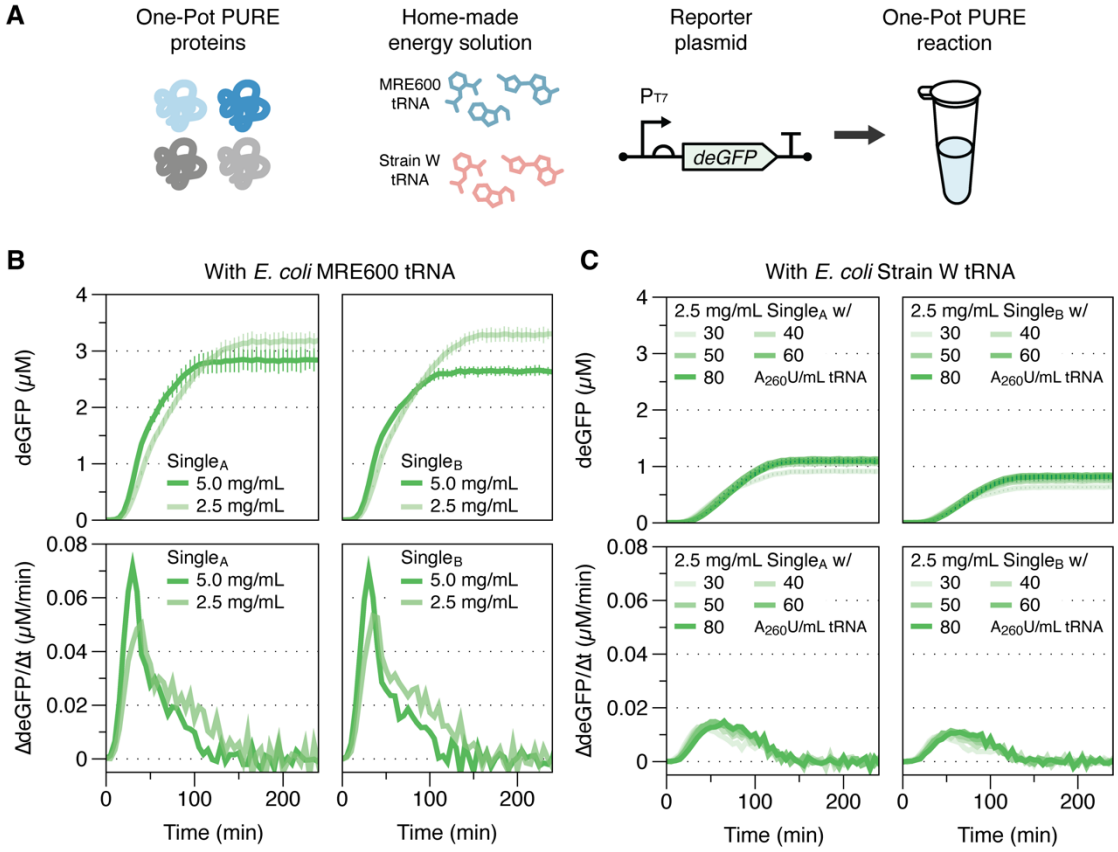


390

391 **Figure 7: (A)** Schematic of One-Pot PURE reaction composition using in-house prepared energy solutions with
392 commercial tRNAs from *E. coli* MRE600 and *E. coli* Strain W. Each reaction contained 5 nM $P_{T7}$-UTR1-deGFP to

393 assess protein production. **(B)** Comparison of deGFP yield and production rate for two batches of Single Strain One-
394 Pot PURE proteins (added to the reaction either at 2.5 or 5.0 mg/mL) in energy solution with 22 $A_{260}$U/mL *E. coli*
395 MRE600 tRNA. Error bars represent standard deviations of reaction triplicates. Protein production rate plots represent
396 the average of reaction triplicates. **(C)** Comparison of deGFP yield and production rate for two batches of Single Strain
397 One-Pot PURE proteins (added to the reaction at 2.5 mg/mL) in energy solution with increasing *E. coli* Strain W tRNA
398 activity units (30 – 80 $A_{260}$U/mL). The plots represent the average of reaction triplicates, and the error bars represent
399 standard deviations of reaction triplicates. Protein production rate plots represent the average of reaction triplicates.

## CONCLUSION

In this work, we identified several important factors that affect the expression capacity of the One-Pot PURE system. We improved the stability of One-Pot PURE protein expression through glucose-mediated catabolite repression and mitigated potential protease degradation from M15/pREP4 expression strains by consolidating all protein expression vectors to one *E. coli* BL21(DE3) strain. This new single-strain approach also increased the expression levels of critical translation initiation and energy regeneration proteins and, consequently, the productivity of the One-Pot PURE reaction. Our characterizations of both dual and single-strain One-Pot PURE proteins in two commercial PURE energy solutions revealed that optimizing biochemical compositions could overcome deficiencies in translation capacity. Lastly, our in-house energy solution preparation revealed the critical role of tRNA composition in determining the translation capacity of PURE reactions.

These findings showcased that the gene expression capacity of the PURE system is influenced by both PURE protein stoichiometry and biochemical factors. At the protein level, we found that when translation initiation factors (initiation factors 2 and 3, IF2 and IF3) and energy regeneration protein, creatine kinase (CK) are present at higher concentrations in the PURE protein mixture, higher expression capacity is observed (**Figure 5D, E**).

At the biochemical level, we found that energy solution composition significantly impacts the One-Pot PURE production rate and the final protein yield. Using the $PURE_A$ energy solution, the reaction proceeded with a slower protein production rate and took over 6 hours to stabilize to the final deGFP concentration (**Figure SI.III 8**). This suggests that there may be a reaction rate-limiting step imposed by the $PURE_A$ energy solution, and this limitation can make One-Pot PURE proteins with sub-optimal protein composition proceed even more slowly, resulting in lower protein yield. On the other hand, the $PURE_B$ energy solution supports a faster protein production rate overall, with reactions completed in under 3 hours (**Figure SI.III 9**). This suggests the rate-limiting step observed in the $PURE_A$ energy solution may be removed in $PURE_B$ to deliver a high protein yield with a shorter reaction lifetime. We hypothesize this rate-limiting step can be the reaction's tRNA composition. We also note that $PURE_A$ and $PURE_B$ energy solutions are proprietary information from commercial vendors. The exact compositions of these energy solutions are not known to us, which limits the conclusions we can draw.

Lastly, we show that commercial preparations of *E. coli* tRNA sourced from strain MRE600 and strain W significantly impact effective protein translation (**Figure 7**). Although MRE600 is a highly preferred source for *E. coli* tRNA due to the strain's low RNase I activity,[42] there is no apparent reason behind tRNA obtained from strain W (a safe and fast-growing strain utilizing sucrose as an industrially preferred carbon source)[43] exhibiting sub-optimal translation capacity. This highlights a critical limitation and source of variability in most cell-free systems (lysate-based and PURE), which is that *E. coli* tRNA is also a complex mixture and exhibits differential concentration profiles across growth stages and host strains.[44,45] For robust control over both One-Pot PURE reaction and potentially lysate-based cell-free expression systems, a promising approach can be developing an optimal tRNA composition.[46]

Taken together, this work seeks to obtain a comprehensive understanding of the factors influencing the gene expression capacity of the One-Pot PURE system. By addressing both protein and biochemical composition, our findings offer valuable insights into optimizing not only

443 One-Pot PURE systems but also extending to lysate-based cell-free protein synthesis, paving the
444 way for more efficient and reliable applications in synthetic biology and biotechnology.

445 **MATERIALS AND METHODS**

446 ***Escherichia coli strains and plasmids***

447 *E. coli* BL21(DE3) (Thermo Scientific) and M15/pREP4 (Qiagen) strains were used for protein
448 expression. **Supplementary Information I** contains the Addgene catalog numbers and plasmid
449 sequences for Dual-Strain One-Pot. To establish the Single Strain One-Pot, all proteins were
450 amplified via Gibson Assembly and placed onto the pET21a backbone. All sequences of cloned
451 proteins transplanted onto pET21a are provided in **Supplementary Information I**.

452 Sequence-verified plasmids (Primordium Labs, now Plasmidsaurus) were transformed into their
453 respective BL21(DE3) and M15/pREP4 expression strains and plated on Luria Broth (LB) Agar
454 plates with 100 $\mu$g/mL carbenicillin and 1% glucose. An inoculation loop was used to scrape
455 multiple colonies to inoculate overnight culture in LB with 100 $\mu$g/mL carbenicillin and 1% glucose
456 to obtain the population expression average. To facilitate inoculation of subsequent final cultures,
457 250 $\mu$L of overnight cultures were saved into frozen glycerol stocks with 250 $\mu$L of 50% glycerol
458 in 1.3 mL 96 well plates (NEST Biotech). The glycerol stock plate was sealed with an aluminum
459 film and stored at -80 ˚C.

460 Sequences of plasmid DNA used for reporter protein expression are provided in **Supplementary**
461 **Information I**. All plasmid DNA was prepared using the NucleoBond Xtra Midi kit (Macherey-
462 Nagel) and eluted in nuclease-free water.

463 ***Monoculture Expression assay for One-Pot PURE proteins***

464 The protocol was adapted from Grasemann *et al.*[27] with a few modifications. An overnight culture
465 of One-Pot PURE protein expression strains was inoculated either from freshly transformed cells
466 grown on LB agar plates with carbenicillin (without or with 1% w/v glucose to exert catabolite
467 repression) or from frozen glycerol stocks using a cryo-replicator (Enzyscreen, CR1000). The
468 overnight culture was grown in 96-well deep-well plates sealed with a Breathe-Easier membrane
469 (Diversified Biotech) at 37 ˚C and 1000 rpm.

470 The next morning, a fresh starter culture was prepared using 4 $\mu$L of the overnight cells and 396
471 $\mu$L of LB with carbenicillin. OD600 was monitored at the time of 0.1 mM IPTG induction to initiate
472 protein expression after 2-2.5 hrs of growth and 3 hours after protein expression. 10 $\mu$L of cells
473 expressing One-Pot PURE proteins were mixed with Lammeli Buffer (Bio-Rad) and heat
474 denatured at 95 ˚C for 10 minutes, and 10 $\mu$L of the mixture was loaded onto Bolt™ 4-12% Bis-
475 Tris Protein Gels (Invitrogen) along with protein ladders (SeeBlue™ Plus2 Pre-stained Protein
476 Standard, Invitrogen). Samples were run at 150 kV, 400 mAmp for 30 minutes with NuPAGE MES
477 SDS buffer (Invitrogen).

478 The gel was stained with SimplyBlue Safe Stain (Invitrogen) for 1 hour and de-stained in water
479 overnight before imaging on a ChemiDoc Imager (Bio-Rad) or a GelDoc Go Imager (Bio-Rad).
480 The obtained protein gel images were analyzed using the accompanying software Image Lab 6.1
481 for Mac (Bio-Rad).

482 ***One-Pot PURE reaction assembly and data acquisition***

483 Detailed methods describing the preparation of One-Pot PURE protein mixture and energy
484 solution are provided in **Supplementary Information II**.

485 All One-Pot reactions were assembled on ice using low protein-binding microcentrifuge tubes
486 (Eppendorf). Each reaction is 5 $\mu$L in total volume and consists of 2 $\mu$M *E. coli* Ribosome (NEB),
487 5 nM reporter protein expression plasmids (either $P_{T7}$-MGA-UTR1-deGFP or $P_{T7}$-UTR1-deGFP),
488 2.5x Energy Solution (125 mM HEPES-KOH pH 7.6, 250 mM Potassium L-Glutamate, 5 mM ATP
489 and GTP at pH 7.5, 2.5 mM UTP and CTP at pH 7.5, either 56 $A_{260}$U/mL for *E. coli* MRE600 tRNA
490 or 75 – 200 $A_{260}$U/mL for *E. coli* W tRNA, 50 mM Creatine Phosphate, 2.5 mM TCEP, 50 $\mu$M
491 Folinic Acid, 5 mM Spermidine, and 0.75 mM amino acids mixture at pH 7.5), 1.75 – 5 mg/mL of
492 One-Pot PURE proteins and 0.5 – 1 $\mu$M T7 RNAP (only for Single Strain One-Pot). For reactions
493 using malachite green aptamer (MGA) fluorescence as a proxy for mRNA transcripts, 10 $\mu$M of
494 malachite green dye was added to the reaction.

495 Following assembly, 5 $\mu$L of each reaction was pipetted onto a low-volume 384-well microplate
496 with a non-binding surface (Corning), and the reaction trajectory was measured every 5 minutes
497 using the BioTek Synergy Plate Reader at 37 ˚C. Fluorescence for deGFP was measured at
498 485/515 nm excitation/emission wavelengths at Gain 61, and fluorescence for malachite green
499 aptamer was measured at 610/650 nm excitation/emission wavelengths at Gain 150. The
500 fluorescence data for MGA and deGFP were calibrated to protein concentration data using
501 synthesized MGA RNA and deGFP protein standards, provided in **Supplementary Information**
502 **III**, **Figure SI.III.10**.

503 ***Acquisition and analysis of proteomics data***

504 A brief summary of LC-MS/MS workflow is provided below. Detailed methods are provided in
505 **Supplementary Information II**.

506 LC-MS/MS analyses of the digested peptides were performed on an EASY-nLC 1200 (Thermo
507 Fisher Scientific) coupled to a Q Exactive HF hybrid quadrupole-Orbitrap mass spectrometer
508 (Thermo Fisher Scientific). MS2 fragmentation spectra were searched with Proteome Discoverer
509 SEQUEST (version 2.5; Thermo Scientific, Waltham, MA) against an *in silico* tryptic digested *E.*
510 *coli* BL21 (DE3) and *E. coli* M15 database. The relative abundance of parental peptides was
511 calculated by integrating the area under the curve of the MS1 peaks.

512 The proteomics data presented in this manuscript are from the same batch of LC-MS/MS run for
513 results to be comparable. The relative protein abundances for each sample are first normalized
514 by scaling the total sample protein abundance with the average total protein abundance for all
515 samples. The proteins involved in the PURE system were extracted from the entire proteome
516 dataset and scaled by their composition in PURE reactions (manufacturer's recommended
517 compositions for $PURE_A$ and $PURE_B$, 4 mg/mL for Dual Strain One-Pot PURE batches A and B
518 in **Figure 2**, and 2.5 mg/mL for all Dual- and Single Strain One-Pot PURE batches A and B in
519 **Figure 5**)

520 ***Characterization of protease activity in M15/pREP4 and BL21/pREP4 strain***

521 Plasmid expressing T7 RNAP (Addgene# 124128) is co-transformed into M15 and BL21 cells
522 with pREP4 plasmid coding for constitutive LacI expression. Transformants were grown in a 5 mL
523 overnight culture with LB with antibiotics and 1% glucose. 1 mL of the overnight was used to start

524 the 150 mL final culture with LB and antibiotics. When culture OD exceeded 0.8, 1 mM IPTG was
525 used to induce T7 RNAP expression, and the culture was grown for an additional 3 hours. At
526 harvest, the cultures were divided into 50 mL aliquots, centrifuged at 5000 x g for 20 minutes to
527 obtain cell pellets, and the pellets were stored at -80 ˚C until use. One 100 $\mu$L aliquot of the M15
528 and BL21 cultures were saved as un-lysed controls.

529 To characterize M15 proteolysis during protein purification, each of the cell pellets was
530 resuspended in 1 mL of the Lysis Buffer (50 mM HEPES-KOH pH 7.6, 100 mM $NH_4Cl$, 500 mM
531 NaCl, 10 mM $MgCl_2$, and 1 mM TCEP). Two variations of the lysis buffer were prepared: one
532 Pepstatin A (1 µg/mL), and another with cOmplete™ Mini, EDTA-free protease inhibitor at the
533 recommended working concentration. The resuspended cells were lysed using the freeze-thaw
534 method by alternating between flash freezing in liquid nitrogen and thawing in a room-temperature
535 water bath 8 times. The lysate was centrifuged at 15,000 rpm at 4°C for 20 minutes to remove
536 cellular debris before His-tag purification.

537 A 2 mL column (Thermo Scientific) was prepared with 200 µL of Ni-Sepharose resin (Cytiva) and
538 equilibrated using 15 mL of Wash Buffer (50 mM HEPES-KOH pH 7.6, 100 mM $NH_4Cl$, 500 mM
539 NaCl, 10 mM $MgCl_2$, 1 mM TCEP, and 20 mM Imidazole-HCl pH 7). Following equilibration, the
540 lysate-resin mixture was rocked at 4 °C for 1 hour to enhance protein binding to the resin, washed
541 with 20 mL of Wash Buffer, and eluted with 250 µL of Elution Buffer (50 mM HEPES-KOH pH 7.6,
542 100 mM $NH_4Cl$, 500 mM NaCl, 10 mM $MgCl_2$, 1 mM TCEP, and 500 mM Imidazole-HCl pH 7).
543 The un-lysed cell culture aliquots, as well as purified proteins from M15 and BL21 strains, were
544 then prepared for SDS-PAGE analysis using the same setting described in the previous sections.

## AUTHOR CONTRIBUTIONS

*Conceptualization:* YZ, RMM, PSF, TC.; *Investigation:* YZ, MD, YQ, LB, ZAM; *Analysis:* YZ, MD, YQ, LB, ZAM; *Writing – manuscript:* YZ, MD, LB, ZAM; *Writing – review and editing:* YZ, MD, RMM, PSF, LB, ZAM, YQ, TC; *Visualization:* YZ, MD, LB, ZAM; *Supervision:* RMM, PSF, TC.


## FUNDING

RMM and YZ are supported by the National Science Foundation, award MCB-2152267, and Schmidt Futures, grant number 2023-3-2-1. YZ is also supported by the Caltech Presidential Postdoctoral Fellowship. PSF and MD are supported by the Engineering and the Physical Sciences Research Council (EPSRC), award EP/T013788/1. MD is also supported by the EPSRC Centres for Doctoral Training in Biodesign Engineering at Imperial College London. LB is supported by the Caltech Summer Undergraduate Research Fellowship (SURF).

## ACKNOWLEDGEMENT

We sincerely thank the Murray Lab members, particularly Dr. Zoila Jurado and Miryong (Miki) Yun, who contributed to the project's early setup and discussions. We also thank b.next, a company working on open-source synthetic cell protocols (https://bnext.bio), for insightful discussions on the 36-Pot PURE preparation. We also thank Dr. Jurado, Manisha Kapasiawala, and Dr. John Marken for their review and feedback on this manuscript.

Dr. Jurado prepared the $P_{T7}$-MGA-UTR1-deGFP plasmid [47] used in this work. We thank Prof. Lulu Qian for access to the ChemiDoc Imager used for protein gel image acquisition. We thank the Caltech Protein Expression Center (PEC) for preparing the purified T7 RNAP used in this work.


## CONFLICT OF INTEREST

R.M.M. has a financial stake in Tierra Biosciences, a private company that uses bacterial lysate-based cell-free technologies for protein expression and screening.

## REFERENCES


(1) Hunt, A. C.; Vögeli, B.; Hassan, A. O.; Guerrero, L.; Kightlinger, W.; Yoesep, D. J.; Krüger, A.; DeWinter, M.; Diamond, M. S.; Karim, A. S.; Jewett, M. C. A Rapid Cell-Free Expression and Screening Platform for Antibody Discovery. *Nat. Commun.* **2023**, *14* (1), 3897. https://doi.org/10.1038/s41467-023-38965-w.

(2) Swank, Z.; Maerkl, S. J. CFPU: A Cell-Free Processing Unit for High-Throughput, Automated In Vitro Circuit Characterization in Steady-State Conditions. *BioDesign Res.* **2021**, *2021*, 2968181. https://doi.org/10.34133/2021/2968181.

(3) Tabuchi, T.; Yokobayashi, Y. High-Throughput Screening of Cell-Free Riboswitches by Fluorescence-Activated Droplet Sorting. *Nucleic Acids Res.* **2022**, *50* (6), 3535–3550. https://doi.org/10.1093/nar/gkac152.

(4) Martin, R. W.; Des Soye, B. J.; Kwon, Y.-C.; Kay, J.; Davis, R. G.; Thomas, P. M.; Majewska, N. I.; Chen, C. X.; Marcum, R. D.; Weiss, M. G.; Stoddart, A. E.; Amiram, M.; Ranji Charna, A. K.; Patel, J. R.; Isaacs, F. J.; Kelleher, N. L.; Hong, S. H.; Jewett, M. C. Cell-Free Protein Synthesis from Genomically Recoded Bacteria Enables Multisite Incorporation of Noncanonical Amino Acids. *Nat. Commun.* **2018**, *9* (1), 1203. https://doi.org/10.1038/s41467-018-03469-5.

(5) Ngo, P. H. T.; Ishida, S.; Busogi, B. B.; Do, H.; Ledesma, M. A.; Kar, S.; Ellington, A. Changes in Coding and Efficiency through Modular Modifications to a One Pot PURE System for In Vitro Transcription and Translation. *ACS Synth. Biol.* **2023**, *12* (12), 3771–3777. https://doi.org/10.1021/acssynbio.3c00461.

(6) Zhang, Y.; Kojima, T.; Kim, G.-A.; McNerney, M. P.; Takayama, S.; Styczynski, M. P. Protocell Arrays for Simultaneous Detection of Diverse Analytes. *Nat. Commun.* **2021**, *12* (1), 5724. https://doi.org/10.1038/s41467-021-25989-3.

(7) Manzer, Z. A.; Ghosh, S.; Jacobs, M. L.; Krishnan, S.; Zipfel, W. R.; Piñeros, M.; Kamat, N. P.; Daniel, S. Cell-Free Synthesis of a Transmembrane Mechanosensitive Channel Protein into a Hybrid-Supported Lipid Bilayer. *ACS Appl. Bio Mater.* **2021**, *4* (4), 3101–3112. https://doi.org/10.1021/acsabm.0c01482.

(8) Thakur, M.; Breger, J. C.; Susumu, K.; Oh, E.; Spangler, J. R.; Medintz, I. L.; Walper, S. A.; Ellis, G. A. Self-Assembled Nanoparticle-Enzyme Aggregates Enhance Functional Protein Production in Pure Transcription-Translation Systems. *PLOS ONE* **2022**, *17* (3), e0265274. https://doi.org/10.1371/journal.pone.0265274.

(9) Luo, S.; Adam, D.; Giaveri, S.; Barthel, S.; Cestellos-Blanco, S.; Hege, D.; Paczia, N.; Castañeda-Losada, L.; Klose, M.; Arndt, F.; Heider, J.; Erb, T. J. ATP Production from Electricity with a New-to-Nature Electrobiological Module. *Joule* **2023**, *7* (8), 1745–1758. https://doi.org/10.1016/j.joule.2023.07.012.

(10) Jung, J. K.; Alam, K. K.; Verosloff, M. S.; Capdevila, D. A.; Desmau, M.; Clauer, P. R.; Lee, J. W.; Nguyen, P. Q.; Pastén, P. A.; Matiasek, S. J.; Gaillard, J.-F.; Giedroc, D. P.; Collins, J. J.; Lucks, J. B. Cell-Free Biosensors for Rapid Detection of Water Contaminants. *Nat. Biotechnol.* **2020**, *38* (12), 1451–1459. https://doi.org/10.1038/s41587-020-0571-7.

(11) Zhang, Y.; Steppe, P. L.; Kazman, M. W.; Styczynski, M. P. Point-of-Care Analyte Quantification and Digital Readout via Lysate-Based Cell-Free Biosensors Interfaced with Personal Glucose Monitors. *ACS Synth. Biol.* **2021**, *10* (11), 2862–2869. https://doi.org/10.1021/acssynbio.1c00282.

(12) Karlikow, M.; da Silva, S. J. R.; Guo, Y.; Cicek, S.; Krokovsky, L.; Homme, P.; Xiong, Y.; Xu, T.; Calderón-Peláez, M.-A.; Camacho-Ortega, S.; Ma, D.; de Magalhães, J. J. F.; Souza, B. N. R. F.; de Albuquerque Cabral, D. G.; Jaenes, K.; Sutyrina, P.; Ferrante, T.; Benitez, A. D.; Nipaz, V.; Ponce, P.; Rackus, D. G.; Collins, J. J.; Paiva, M.; Castellanos, J. E.; Cevallos,

616 V.; Green, A. A.; Ayres, C.; Pena, L.; Pardee, K. Field Validation of the Performance of Paper-
617 Based Tests for the Detection of the Zika and Chikungunya Viruses in Serum Samples. *Nat.*
618 *Biomed. Eng.* **2022**, *6* (3), 246–256. https://doi.org/10.1038/s41551-022-00850-0.
619 (13) Pardee, K.; Slomovic, S.; Nguyen, P. Q.; Lee, J. W.; Donghia, N.; Burrill, D.; Ferrante, T.;
620 McSorley, F. R.; Furuta, Y.; Vernet, A.; Lewandowski, M.; Boddy, C. N.; Joshi, N. S.; Collins,
621 J. J. Portable, On-Demand Biomolecular Manufacturing. *Cell* **2016**, *167* (1), 248-259.e12.
622 https://doi.org/10.1016/j.cell.2016.09.013.
623 (14) Stark, J. C.; Jaroentomeechai, T.; Moeller, T. D.; Hershewe, J. M.; Warfel, K. F.; Moricz,
624 B. S.; Martini, A. M.; Dubner, R. S.; Hsu, K. J.; Stevenson, T. C.; Jones, B. D.; DeLisa, M. P.;
625 Jewett, M. C. On-Demand Biomanufacturing of Protective Conjugate Vaccines. *Sci. Adv.*
626 **2021**, *7* (6), eabe9444. https://doi.org/10.1126/sciadv.abe9444.
627 (15) Shin, J.; Jardine, P.; Noireaux, V. Genome Replication, Synthesis, and Assembly of the
628 Bacteriophage T7 in a Single Cell-Free Reaction. *ACS Synth. Biol.* **2012**, *1* (9), 408–413.
629 https://doi.org/10.1021/sb300049p.
630 (16) Lavickova, B.; Laohakunakorn, N.; Maerkl, S. J. A Partially Self-Regenerating Synthetic
631 Cell. *Nat. Commun.* **2020**, *11* (1), 6340. https://doi.org/10.1038/s41467-020-20180-6.
632 (17) Godino, E.; López, J. N.; Zarguit, I.; Doerr, A.; Jimenez, M.; Rivas, G.; Danelon, C. Cell-
633 Free Biogenesis of Bacterial Division Proto-Rings That Can Constrict Liposomes. *Commun.*
634 *Biol.* **2020**, *3* (1), 1–11. https://doi.org/10.1038/s42003-020-01258-9.
635 (18) Okauchi, H.; Ichihashi, N. Continuous Cell-Free Replication and Evolution of Artificial
636 Genomic DNA in a Compartmentalized Gene Expression System. *ACS Synth. Biol.* **2021**, *10*
637 (12), 3507–3517. https://doi.org/10.1021/acssynbio.1c00430.
638 (19) Garenne, D.; Beisel, C. L.; Noireaux, V. Characterization of the All-E. Coli Transcription-
639 Translation System myTXTL by Mass Spectrometry. *Rapid Commun. Mass Spectrom.* **2019**,
640 *33* (11), 1036–1048. https://doi.org/10.1002/rcm.8438.
641 (20) Miguez, A. M.; Zhang, Y.; Piorino, F.; Styczynski, M. P. Metabolic Dynamics in Escherichia
642 Coli-Based Cell-Free Systems. *ACS Synth. Biol.* **2021**, *10* (9), 2252–2265.
643 https://doi.org/10.1021/acssynbio.1c00167.
644 (21) Garamella, J.; Marshall, R.; Rustad, M.; Noireaux, V. The All E. Coli TX-TL Toolbox 2.0:
645 A Platform for Cell-Free Synthetic Biology. *ACS Synth. Biol.* **2016**, *5* (4), 344–355.
646 https://doi.org/10.1021/acssynbio.5b00296.
647 (22) Sun, Z. Z.; Hayes, C. A.; Shin, J.; Caschera, F.; Murray, R. M.; Noireaux, V. Protocols for
648 Implementing an Escherichia Coli Based TX-TL Cell-Free Expression System for Synthetic
649 Biology. *JoVE J. Vis. Exp.* **2013**, No. 79, e50762. https://doi.org/10.3791/50762.
650 (23) Matsuura, T.; Tanimura, N.; Hosoda, K.; Yomo, T.; Shimizu, Y. Reaction Dynamics
651 Analysis of a Reconstituted Escherichia Coli Protein Translation System by Computational
652 Modeling. *Proc. Natl. Acad. Sci.* **2017**, *114* (8), E1336–E1344.
653 https://doi.org/10.1073/pnas.1615351114.
654 (24) Jurado, Z.; Pandey, A.; Murray, R. M. A Chemical Reaction Network Model of PURE.
655 bioRxiv August 14, 2023, p 2023.08.14.553301. https://doi.org/10.1101/2023.08.14.553301.
656 (25) Lavickova, B.; Maerkl, S. J. A Simple, Robust, and Low-Cost Method To Produce the
657 PURE Cell-Free System. *ACS Synth. Biol.* **2019**, *8* (2), 455–462.
658 https://doi.org/10.1021/acssynbio.8b00427.
659 (26) Stülke, J.; Hillen, W. Carbon Catabolite Repression in Bacteria. *Curr. Opin. Microbiol.*
660 **1999**, *2* (2), 195–201. https://doi.org/10.1016/S1369-5274(99)80034-4.
661 (27) Grasemann, L.; Lavickova, B.; Elizondo-Cantú, M. C.; Maerkl, S. J. OnePot PURE Cell-
662 Free System. *JoVE J. Vis. Exp.* **2021**, No. 172, e62625. https://doi.org/10.3791/62625.
663 (28) *Nucleus*. Nucleus. https://nucleus.bnext.bio.

(29) Grodberg, J.; Dunn, J. J. ompT Encodes the Escherichia Coli Outer Membrane Protease That Cleaves T7 RNA Polymerase during Purification. *J. Bacteriol.* **1988**, *170* (3), 1245–1253. https://doi.org/10.1128/jb.170.3.1245-1253.1988.
(30) Vandeputte-Rutten, L.; Kramer, R. A.; Kroon, J.; Dekker, N.; Egmond, M. R.; Gros, P. Crystal Structure of the Outer Membrane Protease OmpT from Escherichia Coli Suggests a Novel Catalytic Site. *EMBO J.* **2001**, *20* (18), 5033–5039. https://doi.org/10.1093/emboj/20.18.5033.
(31) Brannon, J. R.; Burk, D. L.; Leclerc, J.-M.; Thomassin, J.-L.; Portt, A.; Berghuis, A. M.; Gruenheid, S.; Le Moual, H. Inhibition of Outer Membrane Proteases of the Omptin Family by Aprotinin. *Infect. Immun.* **2015**, *83* (6), 2300–2311. https://doi.org/10.1128/IAI.00136-15.
(32) McCarter, J. D.; Stephens, D.; Shoemaker, K.; Rosenberg, S.; Kirsch, J. F. Substrate Specificity of the Escherichia Coli Outer Membrane Protease OmpT. *J. Bacteriol.* **2004**, *186* (17), 5919–5925. https://doi.org/10.1128/JB.186.17.5919-5925.2004.
(33) *MEROPS - the Peptidase Database*. https://www.ebi.ac.uk/merops/cgi-bin/pepsum?id=A26.001;type=P (accessed 2024-10-20).
(34) Hwang, B.-Y.; Varadarajan, N.; Li, H.; Rodriguez, S.; Iverson, B. L.; Georgiou, G. Substrate Specificity of the Escherichia Coli Outer Membrane Protease OmpP. *J. Bacteriol.* **2006**, *189* (2), 522. https://doi.org/10.1128/JB.01493-06.
(35) Abramson, J.; Adler, J.; Dunger, J.; Evans, R.; Green, T.; Pritzel, A.; Ronneberger, O.; Willmore, L.; Ballard, A. J.; Bambrick, J.; Bodenstein, S. W.; Evans, D. A.; Hung, C.-C.; O'Neill, M.; Reiman, D.; Tunyasuvunakool, K.; Wu, Z.; Žemgulytė, A.; Arvaniti, E.; Beattie, C.; Bertolli, O.; Bridgland, A.; Cherepanov, A.; Congreve, M.; Cowen-Rivers, A. I.; Cowie, A.; Figurnov, M.; Fuchs, F. B.; Gladman, H.; Jain, R.; Khan, Y. A.; Low, C. M. R.; Perlin, K.; Potapenko, A.; Savy, P.; Singh, S.; Stecula, A.; Thillaisundaram, A.; Tong, C.; Yakneen, S.; Zhong, E. D.; Zielinski, M.; Žídek, A.; Bapst, V.; Kohli, P.; Jaderberg, M.; Hassabis, D.; Jumper, J. M. Accurate Structure Prediction of Biomolecular Interactions with AlphaFold 3. *Nature* **2024**, *630* (8016), 493–500. https://doi.org/10.1038/s41586-024-07487-w.
(36) Muller, D. K.; Martin, C. T.; Coleman, J. E. Processivity of Proteolytically Modified Forms of T7 RNA Polymerase. *Biochemistry* **1988**, *27* (15), 5763–5771. https://doi.org/10.1021/bi00415a055.
(37) Shimizu, Y.; Inoue, A.; Tomari, Y.; Suzuki, T.; Yokogawa, T.; Nishikawa, K.; Ueda, T. Cell-Free Translation Reconstituted with Purified Components. *Nat. Biotechnol.* **2001**, *19* (8), 751–755. https://doi.org/10.1038/90802.
(38) Yadav, S.; Perkins, A. J. P.; Liyanagedera, S. B. W.; Bougas, A.; Laohakunakorn, N. ATP Regeneration from Pyruvate in the PURE System. bioRxiv September 8, 2024, p 2024.09.06.611674. https://doi.org/10.1101/2024.09.06.611674.
(39) Bicknell, A. A.; Reid, D. W.; Licata, M. C.; Jones, A. K.; Cheng, Y. M.; Li, M.; Hsiao, C. J.; Pepin, C. S.; Metkar, M.; Levdansky, Y.; Fritz, B. R.; Andrianova, E. A.; Jain, R.; Valkov, E.; Köhrer, C.; Moore, M. J. Attenuating Ribosome Load Improves Protein Output from mRNA by Limiting Translation-Dependent mRNA Decay. *Cell Rep.* **2024**, *43* (4). https://doi.org/10.1016/j.celrep.2024.114098.
(40) Shin, J.; Noireaux, V. Efficient Cell-Free Expression with the Endogenous E. Coli RNA Polymerase and Sigma Factor 70. *J. Biol. Eng.* **2010**, *4* (1), 8. https://doi.org/10.1186/1754-1611-4-8.
(41) Doerr, A.; Foschepoth, D.; Forster, A. C.; Danelon, C. In Vitro Synthesis of 32 Translation-Factor Proteins from a Single Template Reveals Impaired Ribosomal Processivity. *Sci. Rep.* **2021**, *11* (1), 1898. https://doi.org/10.1038/s41598-020-80827-8.
(42) Kurylo, C. M.; Alexander, N.; Dass, R. A.; Parks, M. M.; Altman, R. A.; Vincent, C. T.; Mason, C. E.; Blanchard, S. C. Genome Sequence and Analysis of Escherichia Coli MRE600,

a Colicinogenic, Nonmotile Strain That Lacks RNase I and the Type I Methyltransferase, EcoKI. *Genome Biol. Evol.* **2016**, *8* (3), 742–752. https://doi.org/10.1093/gbe/evw008.

(43) Archer, C. T.; Kim, J. F.; Jeong, H.; Park, J. H.; Vickers, C. E.; Lee, S. Y.; Nielsen, L. K. The Genome Sequence of E. Coli W (ATCC 9637): Comparative Genome Analysis and an Improved Genome-Scale Reconstruction of E. Coli. *BMC Genomics* **2011**, *12* (1), 9. https://doi.org/10.1186/1471-2164-12-9.

(44) Dong, H.; Nilsson, L.; Kurland, C. G. Co-Variation of tRNA Abundance and Codon Usage in Escherichia Coli at Different Growth Rates. *J. Mol. Biol.* **1996**, *260* (5), 649–663. https://doi.org/10.1006/jmbi.1996.0428.

(45) Wei, Y.; Silke, J. R.; Xia, X. An Improved Estimation of tRNA Expression to Better Elucidate the Coevolution between tRNA Abundance and Codon Usage in Bacteria. *Sci. Rep.* **2019**, *9* (1), 3184. https://doi.org/10.1038/s41598-019-39369-x.

(46) Maheshwari, A. J.; Calles, J.; Waterton, S. K.; Endy, D. Engineering tRNA Abundances for Synthetic Cellular Systems. *Nat. Commun.* **2023**, *14* (1), 4594. https://doi.org/10.1038/s41467-023-40199-9.

(47) Jurado, Z.; Murray, R. M. Impact of Chemical Dynamics of Commercial PURE Systems on Malachite Green Aptamer Fluorescence. bioRxiv March 26, 2024, p 2024.03.15.585317. https://doi.org/10.1101/2024.03.15.585317.